Research Article
doi: 10.1590/01047760202430013320
vol(30), 2024

CERNE

The dispersibility of Cellulose I and Cellulose II by tempo-mediated oxidation

Nursyamimi Ahmad Ghazali[1], Kushairi Mohd Salleh[2,3*], Nur Fathihah Jafri[1], Khairunnisa Atiqah Mohamad Khalid[1], Sarani Zakaria[1], Nurul Husna Ab Halim[1]

[1]Bioresource and Biorefinery, School of Applied Physics, Faculty of Science and Technology, Universiti Kebangsaan Malaysia, Selangor Malaysia
[2]Bioresource Technology Division, School of Industrial Technology, Universiti Sains Malaysia, Malaysia
[3]Renewable Biomass Transformation Cluster, School of Industrial Technology, Universiti Sains Malaysia, Malaysia

ABSTRACT

Background: The restricted dispersibility of cellulose in water has grown to be a significant problem which is a key step in making cellulose soluble in water and common solvent. To overcome the obstacle, cellulose structure is being modified to improve the surface properties and the utilization of the cellulose itself. In this study, cellulose I and cellulose II were examined after treated with water-soluble 2,2,6,6-tetramethylpiperidine-1-oxyl radical (TEMPO). The hydrogen bond between chains and the crystallinity of the cotton linter (cellulose I) was first broken by NaOH/urea. Then, cellulose I and NaOH/urea-treated cellulose (cellulose II) were oxidized with sodium chlorite, sodium bromide, and TEMPO in a catalytic amount.

Results: The success of oxidation is achieved when both cellulose I and II treated with TEMPO had preferentially converted the hydroxyl groups to carboxylate groups through Fourier Transform Infrared Spectrometer (FTIR). Besides, through X-ray diffraction analysis, cellulose I and II exhibited a decreased in the crystallinity. The scattered structure revealed through morphology analysis proved that cellulose treated with TEMPO had resulted in a more dispersed and separated cellulose fibre structure.

Conclusion: The result showed, cellulose has been successfully modified using TEMPO-mediated oxidation with improved dispersion properties. The scattered structure revealed through morphology analysis proved that cellulose treated with TEMPO had resulted in a more dispersed and separated cellulose fibre structure. High cellulose dispersion ability will allow the manufacturing process of hydrogel, film and fibre to be much easier and faster. This is necessary for creating novel, environmentally friendly materials for various applications across numerous industries and future research anticipated to increase.

Keywords: 2,2,6,6-tetramethylpiperidine-1-oxyl radical; Bioresource based products; Carboxyl groups; Cellulose solubility; Crystallinity; Dissolution.

HIGHLIGHT

2,2,6,6-tetramethylpiperidine-1-oxyl radical (TEMPO) can modified cellulose with different molecular orientation (cellulose I and cellulose II)
New functional group (-COOH) appeared after TEMPO oxidation has affected the crystalline structure of cellulose
TEMPO-modified cellulose experienced thermal degradation at lower temperature
Cellulose II-TEMPO is observed to have the highest stability and dispersibility with enhanced fibers dispersion and separation.

GHAZALI, N. A.; SALLEH, K. M.; JAFRI, N. F.; KHALID, K. A. M.; ZAKARIA, S.; HALIM, N. H. A. The dispersibility of Cellulose I and Cellulose II by tempo-mediated oxidation. CERNE, 2024, v30, e-103320, doi: 10.1590/01047760202430013320.

✤Corresponding author: kmsalleh@usm.my Received: August 15/2023 Accepted: February 27/2024

Open Access
CERNE
ISSN 0104-7760
UFLA UNIVERSIDADE FEDERAL DE LAVRAS

INTRODUCTION

Cellulose is the most bounteous and sustainable biopolymer on the planet. It comprises unbranched polysaccharide units of -1,4-linked d-glucose and organize in both crystalline and amorphous regions (Ilham 2022). It has been employed by most researchers and industry members for ages because of its sustainable, environmentally friendly, and non-toxic sources (Padzil et al. 2015). Native cellulose (cellulose I), which naturally occurs in plant cell walls, has a highly ordered orientation (crystallinities) and is composed of parallel strand alignment. By dissolving and mercerized, cellulose I can be transformed into cellulose II. As opposed to cellulose I, cellulose II consists of antiparallel strains with intersheet hydrogen bonding and exhibits greater thermodynamic stability (Gubitosi et al. 2017; Nunes 2017). Moreover, it has been widely acknowledged in the past decade that cellulose II is the most easily digestible polymorph of cellulose with its modified lattice pattern and reduce in crystallinity (Nagarajan et al. 2017). For that reason, the study on cellulose I and cellulose II frequently attracts the attention of most researchers due to the difference in the arrangement of hydrogen bond networks that can be used as a comparison in any study conducted.

Cellulose dispersibility and solubility is the key to the problem in its applications. Direct use of cellulose is still limited due to its high molecular weight and highly structured composition such as inter- and intramolecular hydrogen bonding between hydroxy groups of nearby cellulose strands (Ghazali et al. 2022). This made it challenging for cellulose to be dispersed and solubilize in water and most common solvent (Eo et al. 2016; Zhang et al. 2017b). Cellulose with limited dispersibility requires more chemicals and energy to dissolve. The term dispersed describes the process by which the smallest dispersion unit of an aggregate are separated and mixed with the main matrix system (Njuguna, Vanli & Liang 2015a). When all of the accessible cellulose are uniformly distributed in the host matrix, a satisfactory distribution is attained (Zhou et al. 2021). There are several factors consider to improve cellulose dispersibility. This include chemical composition, crystallinity, molecular weight and morphology of cellulose fibers together with its porosities (Krassig HA 1994). Hence, chemical modification of cellulose to alter the refractory structure and its chemistry properties is necessary to increase the cellulose dispersion rates. Chemical alterations such as etherification, esterification, oxidation and grafting are few examples that can modify the features of the cellulose. It is possible to chemically modified cellulose by oxidation method which owns three responsive hydroxyl crowd in its repeating unit (1) primary hydroxyl group (-OH) at C6; (2) secondary hydroxyl group (-OH) at C2 and C3. The introduction of new functional groups, such as carbonyl and carboxyl groups, has led researchers to use oxidation methods particularly frequently (Baron; Coseri, 2020; Coseri et al. 2015).

The TEMPO modification method has been used by many researchers since the idea of making polyglucuronic acid soluble in water was realized (Isogai et al. 1998; Tang et al. 2017). Catalytic oxidation with 2,2,6,6-tetramethylpiperidine-1-oxy radical (TEMPO) is the most straightforward and efficient oxidation technique for adding carboxylic functionality into cellulose fibres (Milanovic et al. 2020). After introducing a stable nitroxyl radical mentioned as TEMPO, the C6-OH groups of the primary hydroxyl located on the surface of cellulose are slowly transformed into -COOH groups through selective oxidation. This process leads to producing products that possess greater hydrophilicity, making them more compatible with water and easily soluble (Baron; Coseri, 2020). The TEMPO oxidation allowed native cellulose to be completely distributed in water down to elementary fibrils. After the cellulose is dispersed, the solvent can reach the exposed cellulose surface and in-contact with it, cause solubilization. The TEMPO technique of oxidation inserts sodium carboxy groups on the surface of cellulose primary fibrils and oxidize polysaccharides (Kaffashsaie et al. 2021; Saito et al. 2006). Over recent decades, TEMPO modification technique have made valuable contributions to the study on native cellulose (cellulose I). However, long crystalline microfibrils with high molecular weight of cellulose I are generally difficult to be dispersed in water. According to past research, there was a previous study to reduce the molecular weight of cellulose using acid hydrolysis. However, acid hydrolysis of cellulose breaks it down into smaller pieces with reduced chain length (Rohaizu & Wanrosli 2017; Shen et al. 2017). Also, it may not significantly improve the dispersibility properties of cellulose. This hinders the subsequent process of cellulose regeneration because the molecular weight of the cellulose is too low with shorter cellulose fibers.

A key element of cellulose's industrial applications and potential future uses is its dispersion. Dispersion makes cellulose more soluble in a wider variety of solvents, increasing its adaptability and opening up new applications. With the introduction of the negative charges to cellulose by TEMPO-oxidation, it exhibits a strong dispersing effect in water and other polar solvents. This dispersion stability is essential for successful integration in a variety of applications where uniform dispersion of cellulose is essential to improve material properties. For instance, in agricultural applications such as hydrogel for control release fertilizer, the dispersion properties of cellulose are needed to improve product performance. The excellent dispersion rate of the cellulose lead to a wide and uniform dispersion in the hydrogel matrix. This is necessary to control the release of fertilizers and other nutrients evenly over time (Beck, Bouchard, Berry, 2012; Chaka, 2022). Furthermore, the dispersibility of cellulose also make it useful for biomedical applications such as drug delivery and tissue engineering. Good cellulose dispersion improves the quality of the final material and helps ensure the incorporation into the desired material (Joseph et al. 2020). Therefore, in this study, the dispersibility and effect of cellulose I and cellulose II by TEMPO-mediated oxidation is being studied. To the best of authors' knowledge, TEMPO-oxidation modification on cellulose II (alkali/urea treated cellulose) notably its physical and thermal characterization has been rarely reported. Theoretically, cellulose II with TEMPO modification has

higher probability of increasing its dispersion rates due to their higher amorphous region and stable arrangement of cellulose (Gubitosi et al. 2017). With the transformation from hydroxy group (-OH) in cellulose to carboxyl groups (-COOH), it is expected that TEMPO modified cellulose will have greater dispersion ability.

MATERIAL AND METHODS

Materials

Pure cotton linter was obtained from Hubei Chemical Fiber (Xiangfan, China). Sodium hypochlorite (NaClO) with 8 wt.% concentration was purchased from Acros Organics. Sodium hydroxide (NaOH), urea, 2,2,6,6-tetramethylpiperidine-1-oxy (TEMPO) and sodium bromide (NaBr) were provided by Sigma Aldrich. All chemicals will be used without further purification.

Preparation of Cellulose II

Pure cotton linters are marked as cellulose I (C1). To obtain cellulose II (C2), 1 g amount of C1 was dissolved in 100 mL NaOH/urea/water solution with a ratio of 7:12:81 at -13°C under vigorous stirring. After being dissolved, the cellulose solution was centrifuged at 8,000 rpm for 10 minutes (to remove air bubbles and separate insoluble contaminants), then the supernatant cellulose solution was dropped into 2 L of water to regenerate the cellulose. Then, cellulose suspension was formed, filtered and rinsed with distilled water few times until neutralized. The suspension was stored in a deep freeze (-41°C) overnight and freeze-dried for 24 hours to obtain Cellulose II (C2).

Preparation of C1-TEMPO and C2-TEMPO

TEMPO-oxidation preparation is adopted from (Tang et al. 2017). TEMPO (0.02 g) with 3.175 g NaBr were added into 125 mL of distilled water, and followed by the dispersion of 1.2 g of cotton linter (C1). The pH of the solution was controlled at pH 10 by adding 0.1 mol/L NaOH solution. Under mild agitation, 28.5 mL of 8 wt. % NaClO solutions was dropped in by drops to initiate the oxidation of cellulose. The reaction time for this process was set for 6 hours with pH of 10 ± 0.5 was maintained throughout the process. The reaction was quenched with the inclusion of 1.25 mL ethanol to the solution. Afterward, the solution was dialyzed in distilled water for two days and freeze-dried to obtain C1-TEMPO.

The same technique mentioned above was performed on C2 to obtain C2-TEMPO. About 1.2 g of C2 obtained was added into 125 mL of distilled water containing 3.175 g NaBr and 0.02 g TEMPO. A 0.1 mol/L NaOH solution was added gradually to keep the solution at pH 10. The cellulose oxidation process begins with the inclusion of 28.5 mL of 8 wt.% NaClO solution. After 6 hours, 1.25 mL of ethanol solution was added to terminate the reaction. The efficiency of TEMPO-mediated oxidation on different cellulose allomorphs was evaluated with further characterizations.

Field Emission Scanning Electron Microscope (FESEM)

The surface morphology of treated cellulose was examined using a field emission scanning electron microscope (FESEM) (Zeiss/Supra 55VP) with an accelerating voltage of 10 kV. Samples were freeze-dried prior to gold coating. All samples were examined under 5000× and 100× magnification (Gan et al. 2017).

X-ray Diffraction (XRD)

X-ray diffraction (Bruker D8 Advance Madison, WI, USA) was used to determine phase changes and crystallinity of C1, C2, C1-TEMPO and C2-TEMPO samples. The XRD was performed with Cu Kα= 1.5405 Å radiation at a diffraction angle of (2) ranging from 5 to 40°. The crystallinity index (CI) was reported using Segal technique to measure the crystallinity values of all samples (Segal et al. 1959). Equation (1) below was used to calculate the Segal CI (%). In which I_t referred to the total intensity of cellulose at peak 2θ = 22.2 which correspond to [200] plane for cellulose I crystal lattice and 2θ = 19.8 for cellulose II, wherein referred to the amorphous intensity, which created by amorphous cellulose between lattice surfaces [101] and [020] (Gao et al. 2020; Nam et al. 2016).

$$CI(\%) = \frac{(I_t - I_a)}{(I_t)} \times 100 \quad (1)$$

Fourier Transform Infrared Spectroscopy (FTIR)

FTIR-Spectrum 400 (Perkin Elmer/BX, USA) was used to identify functional groups changes in C1, C2, C1-TEMPO and C2-TEMPO samples. The samples were first dried, and infrared spectrum analysis scanning was recorded at 32 scans with a resolution of 4 cm^{-1}, and the spectra were obtained in the transmittance mode at ambient temperatures throughout the 4000 – 660 cm^{-1} wavelengths.

Molecular weight (M_η) and degree of polymerization (DP)

The intrinsic viscosity of cellulose before and after TEMPO was determined using an Ubbehlode viscometer of the cadoxen solution in a 30°C water bath. Cadoxen solution was prepared at temperature 0 - 2°C (in ice bath). The solution was then stored overnight in a refrigerator. Filtered the clear solution obtained using filter number 3 and filter number 4 to obtain cadoxen solution. The C1 sample was dissolved in the cadoxen solution at a concentration of 2 × 10^{-3}, and then diluted three times to achieve concentrations

ranging from 5 × 10^{-4} to 2 × 10^{-3} g/mL. The intrinsic viscosity, [η] and Huggin's constant (κ') were estimated using Huggins Equation (2) and Kramer Equation (3) (Gan et al. 2015b). The viscosity of the cellulose samples in cadoxen was then measured, and repeat the same step for C2, C1-TEMPO and C2-TEMPO. Where k'_K and k'_H is a constant for Kraemer and Huggins equations respectively; $\frac{\eta sp}{c}$ represents reduced viscosity and ln $\frac{\eta r}{c}$ represents the inherent viscosity of the cellulose samples.

$$\frac{\eta sp}{c} = [\eta] + k'_K[\eta]^2 c \quad (2)$$

$$ln\frac{\eta r}{c} = [\eta] + k'_H[\eta]^2 c \quad (3)$$

Thermogravimetric and Differential Thermogravimetric Analysis (TGA and DTG)

The thermal properties of all samples were carried out using thermogravimetric analyser, Mettler Toledo (TGA/SDTA 851 e). About 2 – 4 mg sample was conducted in an inert atmosphere of N_2 (50 mL/min) with a heating rate of 10°C/min from 50 to 400°C.

Ultraviolet-visible (UV-Vis) Analysis

The stability of the cellulose was predicted using a UV-Vis absorbance test. Prediction of the stability of cellulose was completed in distilled water at the bottom of the vial bottle during the sedimentation test. The inability of cellulose to disperse well and its low stability will cause the particle to settle to the bottom of the base-fluid. In this work, C1, C2, C1-TEMPO and C2-TEMPO were used. Uv-vis spectrometer (Jenway 7415) was used to perform experiments with 800 nm wavelengths (Zainith; Mishra 2021). The absorbance measured by the spectrometer was being recorded and compared within 90 minutes for each sample.

RESULTS AND DISCUSSION

Morphology of cellulose by FESEM

The FESEM morphology analysis as shown in Figure 1 revealed different structures of cellulose before and after TEMPO modification on both C1 and C2 samples. FESEM images of Figure 1(a) and (b) represent the samples for C1 and C1-TEMPO respectively with 5000× magnifications. As shown in Figure 1a, the surface structure of C1 display an uneven surface structure, while for Figure 1b displays the C1-TEMPO morphology, with the fibrous shape of the C1 can still be preserved, resulting in smoother and even surface structure. As shown by XRD results below, C1 have higher crystallinity which performed a well-structured and highly organized alignment of cellulose chain within the crystal lattice. The uneven surface structure of C1 can be correlated with the long polymer chain of cellulose, which results in dense packaging and the formation of larger, closely interconnected fibre clusters (Bajpai 2016; Sawada et al. 2022). Matched C1 with C1-TEMPO morphology, the average fibre diameter has been seen to reduce after TEMPO modification. The reduced in diameter of fibre might be attributed to the depolymerization of cellulose chains during TEMPO modification (Zhao et al. 2019). Breaking down the cellulose chains into shorter length can potentially diminish the overall size of the cellulose. Furthermore, the beads-like structure noticed on the C1-TEMPO fibre structure might be due to the uneven distribution during modification of TEMPO.

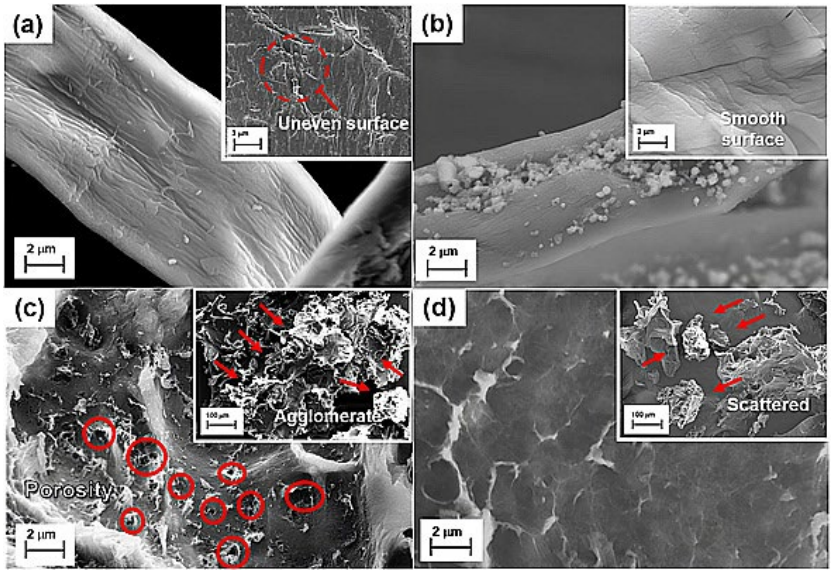

Figure 1: FESEM morphology of (a) C1; (b) C1-TEMPO; (c) C2; (d) C2-TEMPO.

The conversion from C1 to C2 was then developed by dissolving in NaOH/urea solution. The dissolved cellulose chains will unintentionally self-organize during the dissolving of C1 into NaOH/urea, which will result in the rehabilitation of their hydrogen bond structure in a particular way (Tang et al. 2017). For recognizing the morphological features of C2 and C2-TEMPO samples, FESEM was utilized at magnifications of 100×. Solid, dense, rough structures with pores network were observed in Figure 1c. The other way around for C2-TEMPO samples, where it shows solid structure without any pores that can be observed in Figure 1d. The dense structure and increment in porosity noticed in C2 samples reveal that the substance contains pores and voids, probably brought on by NaOH/urea regeneration process (Gan et al. 2015a). Contrarily, lack of pores in C2-TEMPO is due to cellulose rearrangement as discussed in the next XRD section. The rearrangement had caused from a pore structure to a non-pore structure. Other than that, reduced agglomeration or scattered structure detected in C2-TEMPO indicate that TEMPO alteration helped improve the cellulose fibres dispersion and separation, inducing a more uniform and minimally agglomerated structure.

X-ray diffractometry (XRD) analysis

Figure 2 depicts the diffractogram for all samples including the crystallinity percentages stated in the figure. Cellulose is a semi-crystalline structure thus; it is normal to have a low crystalline arrangement in their lattice structure (Alves et al. 2016). In this study, C1 is the main precursor, followed by conversion to C2 via dissolution and regeneration process. According to Figure 2, C1 demonstrates cellulose I formation with the peaks at 2θ = 14.5°, 16.2°, 22.2° and 33.8° with Miller Indices of (1-10), (110), (200) and (004) respectively (Nam et al. 2016). Both cellulose I before (C1) and after TEMPO-treated (C1-TEMPO) maintained the structure with the highest peak of 2θ = 22.2°. After regeneration process (NaOH/ urea treated), the diffraction peaks appeared at 2θ = 12.2°, 19.8° and 21.9° with Miller Indices of (1-10), (110) and (020) peak respectively. All of these peaks were observed in C2 and C2-TEMPO, indicating that the conversion of cellulose I to cellulose II was successful. This also implies that the transition from C1 to C2 involved a number of structural modifications in the cellulose chains. C2 sample has lower crystalline portions of 32.2% with a reduction of 32.7% from C1. The broad peak shows the breaking and destruction of the hydrogen bonds in C1 crystals after dissolving them in NaOH/urea solution (Gan et al. 2016). According to Mazlan et al. (2019), the reduction in the crystallinity index of cellulose is due to the destruction and disturbance of the crystalline area of samples during cellulose dissolution and regeneration process. Besides, the rapid proton exchange of the -OH groups cellulose led to an unrecovered hydrogen bonding network (Zhang et al. 2017b). This process promotes the development of amorphous regions in the C2 samples.

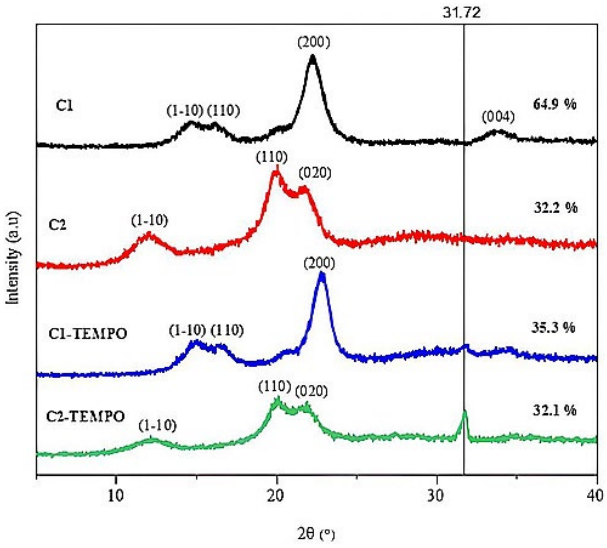

Figure 2: X-ray diffraction (XRD) patterns of unmodified (C1, C2) and modified TEMPO (C1-TEMPO, C2-TEMPO) samples.

Furthermore, changes in the crystallinity portions are expected to be affected after the TEMPO-mediated oxidation process. This statement is guided by the observation in Figure 2 for C1-TEMPO and C2-TEMPO. After TEMPO-mediated oxidation on C1 (C1-TEMPO), the value for CrI has reduced but not for C2-TEMPO. The CrI value for C1-TEMPO has decreased due to the destruction some of inter- and intra- hydrogen bonding of cellulose I during oxidation reaction with TEMPO has taken placed. The destruction is then pursued by unorderly rearrangement of cellulose macromolecule structure via inter- and intramolecular forces (Hastuti et al. 2019; Puangsin et al. 2013). Meanwhile, C2-TEMPO has a similar CrI value with its precursor, even though the graph is marginally different. TEMPO-mediated oxidation did react with the C2 macromolecule but only with the unorderly lattice region. It showed that amorphous regions were exposed to the reaction, not the crystalline area. Owing to this, the CrI value remains constant but with different diffraction of behaviour. Different diffraction behaviour gave C2-TEMPO less intense and new peaks formed for C1-TEMPO and C2-TEMPO at 2θ = 31.72°. It is assumed that the formation of a new peak at 2θ = 31.72° is due to the formation of a new functional group, as mentioned in next FTIR section. The new functional group (-COOH, carboxyl group) that appeared during TEMPO modification has affected the crystalline structure and resulted in new peaks in the XRD pattern.

Fourier Transform Infrared (FTIR) analysis

The characterization and changes of functional group cellulose were analysed using FTIR spectrum. Figure 3 illustrates the major bands in all treated cellulose which can be allocated to 3333 cm^{-1}, 2900 cm^{-1}, 1605 cm^{-1}, 1428 cm^{-1} and 1024 cm^{-1} depending on the functional group present in the

sample. The band located at 3333 cm^{-1} depicts the stretching vibration of a hydroxyl group (-OH) from cellulose, owing to the dampness condition in cellulose samples. The stretching peak at 2900 cm^{-1} shows hybridized C-H stretching that appeared in all samples. The peak for both cellulose I (C1 and C1-TEMPO) can be observed at 1428 cm^{-1} which represent the stretching vibration of C-H, and it is no longer visible during regeneration, indicating that the conversion from cellulose I to cellulose II is successful (Yang et al. 2011). This is most likely due to the disruption and implication of the intermolecular hydrogen bonding that O_6 exocyclic hydroxyl groups were involved in (Gan et al. 2018). The peak at 1024 cm^{-1} in the spectrum exhibits a spectrum of the C-OH stretching of the cellulose backbone (Baron; Coseri, 2020).

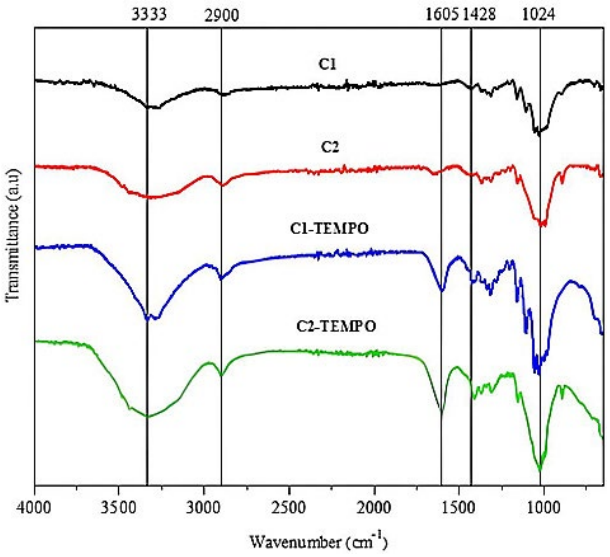

Figure 3: FTIR spectrum of C1, C2, C1-TEMPO and C2-TEMPO.

The most noticeable feature in the oxidised sample (C1-TEMPO and C2-TEMPO) FTIR spectra stipulate a particular functional group inaugurate during the modification procedure. The peak appeared in both C1-TEMPO and C2-TEMPO at 1605 cm^{-1} shows stretching vibration of carbonyl group (C=O) which signifies the D-glucose unit hydroxymethyl group that has provenly converted to carboxyl group (-COOH) in their acidic form (Isogai, et al; 2011; Wang et al. 2022). Through TEMPO-mediated oxidation, the emergence of this change can be attributed to the oxidation process acting on the primary hydroxyl (-OH) groups inherent in the cellulose polymer (Coseri et al. 2015; Hirota et al. 2010; Okita et al. 2010). With the existence of carboxyl group (-COOH), cellulose with TEMPO modification can enhance the hydrophilicity and water absorption capacity for both TEMPO-modified celluloses (Baron; Coseri, 2020; Wang et al. 2022). In contrast to the raw samples, C1-TEMPO and C2-TEMPO show intensity strengthening for both sample which propose the bond enhancing or additional functional group throughout the modification. Relating FTIR and XRD analysis, the intensity strengthening may occur due to the reduction in the crystallinity of TEMPO-modified cellulose samples. This modification will also have an impact on the thermal stability through TGA analysis.

Molecular weight (M_η) and degree of polymerization (DP)

Average molecular weight (Mw) analysis is identified as the technique for measuring the mass of each individual chains, along with determination of total molecular weight polymer (Shrivastava 2018). In this study, the viscosity average molecular weight is employed where the molecular weight of the sample is discovered via viscometer measurement of the cadoxen solution. The concentration and the polymer's molecular weight affect the solution's viscosity. The intrinsic viscosity, [η] to derive the value of the molecular weight, M_η and the degree of polymerization, DP was determined from intrinsic viscosity, [η] using Mark-Houwink equation as expressed in Equation (4) and the degree polymerization (DP) was obtained using Equation (5):

$$[\eta] = 3.85 \times 10^{-2} (M_\eta)^{0.76} (mL\ g^{-1}) \quad (4)$$

$$[\eta] = 1.75 (DP)^{0.69} \quad (5)$$

The result in Table 1 shows the average M_η and the DP of cellulose I (C1) and cellulose II (C2) before and after TEMPO-treated. After treatment with NaOH/urea (C2), the molecular weight decreases by almost 49% compared to C1. As the M_η decreases, the degree of cross-linking between the molecular chains decreases and the diameter of the fiber formed also decreases (Xie et al. 2021). This explanation is supported by Figure 1, where the fiber diameter of C2 is narrower than that of C1. To perform experiments involving dissolution and interaction of cellulose, low molecular weight of cellulose is preferrable. The higher the M_η and the DP of cellulose, the more difficult it is for chemical to reach the crystalline regions of the cellulose (Wang; Deng 2009).

Table 1: The average viscosity molecular weight and degree of polymerization of cellulose I and cellulose II before and after TEMPO-treated.

Sample	Molecular weight, Mη (g/mol)	Degree of polymerization, DP
C1	9.0×10^4	1133.86
C2	4.62×10^4	543.78
C1-TEMPO	3.09×10^4	349.51
C2-TEMPO	2.63×10^4	292.81

Moved on to the next results where, the average viscosity M_η of C1 during the TEMPO oxidation reaction has reduced from 9.0 x 10^4 g/mol (C1) to 3.09 x 10^4 g/mol (C1-TEMPO). During TEMPO oxidation process, the polymer

chains cleaved, into a lower M_η. This is further demonstrated by the DP results, which decreased after both cellulose I and II were treated with TEMPO. It is hypothesized that in the disorganised section, a few glucosidic bond splitting occurred, allowing acid to permeate through and produce a sharp decline in the DP of cellulose through a hydrolysis process. Along with TEMPO modification, the fibre underwent defibrillation and the H^+ ion assistance that caused breaking of the cellulose chain (Padzil et al. 2015). Due to the low entropic driving force from the large molecular weight, the dissolution processed was disrupted. Thus, in order to dissolve cellulose, a powerful solvent is required to break the inter and intra- hydrogen bonding between cellulose microfibrils (Medronho & Lindman 2014). Moreover, the attack of chemicals on the cellulose crystalline area caused it to degrade, which then led to a decrease in gradually M_η to coincide with a decrease in DP. With a decreasing amount of M_η and DP, there is adequate intermolecular entanglement and stronger intermolecular interaction. Low M_η of cellulose had caused an increase in dispersibility and solubility along with decreasing the aggregation of the molecular chain. Additionally, the poor processability of the polymer was brought on by its enormous M_η. As a result, having a low M_η is essential when it significantly affects the cellulose dispersibility and processability (Xie et al. 2021).

Thermal analysis of cellulose

Thermogravimetric analysis (TGA) is used to analyse the thermal behaviour of both C1 and C2 before and after TEMPO-treated. The TGA and their derivative thermo-gravimetry (DTG) curves for all samples are shown in Figure 4(a) and (b), respectively. The small loss occurred at the early stage at temperature up to 25°C along with evaporation produced by adsorbed water in the cellulose sample (Zhang et al. 2017a). In the first stage, decomposition takes place from 25°C until 195°C, where the first stage of the thermal degradation for cellulose without TEMPO-modification (C1 and C2 sample) did not reveal a notable peak. This statement is supported by the DTG graph in Figure 4(b). However, extreme weight loss occurred at level II from 193°C to 386°C. This can also be correlated with the DTG curves shown in Figure 4(b), which showed a significant peak indicating an apparent weight loss, and the peak relocated to the right part with rising cellulose content. The extreme weight loss occurred by simultaneous cellulose-lose degradation processes such as depolymerization of treated cellulose. The obvious peak caused by decomposition temperature, correlates the greatest devolatilization value (Zhao et al. 2019). In level III, the amount of weight loss started to reduce due to the oxidation and degradation of the char residue into lower molecular weight gaseous products (Zhao et al. 2019).

Figure 4(b) display the DTG curves of the peak fluctuations against four varieties of cellulose before and after TEMPO-treated. The DTG curves (Figure 4(b)) of raw cotton linter (C1) shifted towards the right, showing that the degradation temperature of C1 was higher (greater thermal stability) than those of other cellulose types. According to Rubentheren et al. (2016), the crystallinity of the cellulose also exhibited its thermal stability. This is according to C1 samples that are categorized among the higher levels of crystallinity (64.9%) with higher intermolecular hydrogen bonding. This is followed by C2, which has the second highest crystallinity (32.2%) and the second highest thermal stability after C1. Thermal degradation of C2 sample was found to be reduced due to decomposition of the modified crystalline regions (cellulose II) with NaOH/urea solvent (Wei et al. 2020; Zhao et al. 2013).

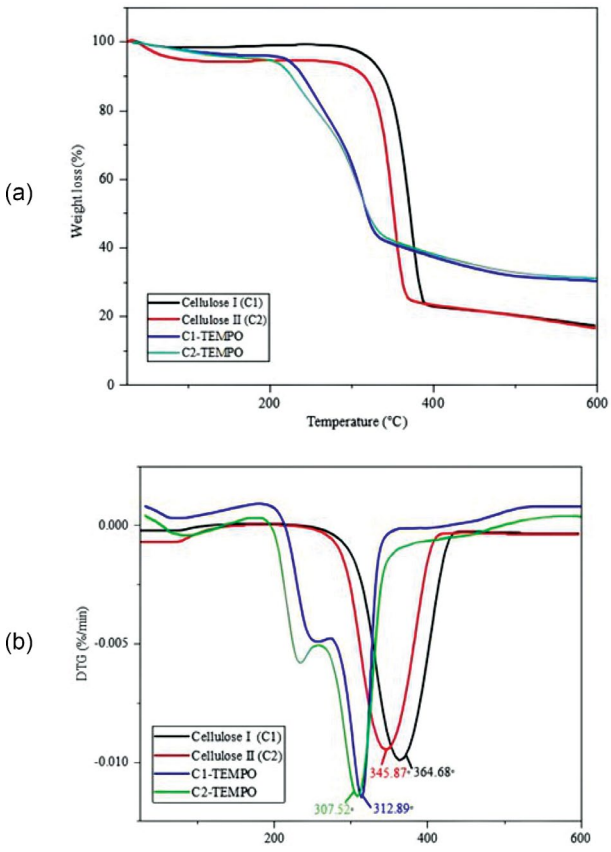

Figure 4: (a) Thermal properties (TGA); (b) DTG of cellulose before and after TEMPO-modified.

However, when oxidized TEMPO was introduced, the thermal stability of the treated cellulose decreased dramatically. TEMPO was found to play an important role in causing the lowest decomposition temperature, indicating low thermal stability. This occurrence is due to the carboxylic functional moiety of the TEMPO-treated cellulose present in C6 groups (Mhd Haniffa et al. 2017). Such thermal instability of oxidized-containing materials is most likely affected by the decarbonation of the anhydro glucuronate units on the surface of oxidized cellulose (Fukuzumi et al. 2010). Briefly, the thermal instability of cellulose after TEMPO-treated is caused by a larger number of reducing (free aldehydes) end groups. It is believed that the thermal stability of cellulose is affected by many elements, involving the origin of cellulose, the crystallinity of cellulose, the oxidation process, which

may significantly alter the thermal features. Position of the -COOH groups on the ring structure, which is directly related to their existence also influenced the thermal stability of cellulose. Into the bargain, the lowest thermal stability of C2-TEMPO is probably due to the thermal stability of dissolved or regenerated cellulose. It has been reported that the onset and maximum thermal decomposition temperatures of regenerated cellulose are 20°C to 50°C lower than those of native cellulose (C1). The cellulose fibers treated with NaOH contained higher fraction of regenerated cellulose fibers, resulting in a reduction of thermal stability. Another explanation is that the sample treated with NaOH were less organized and therefore more vulnerable by heating process as evidenced by their low crystallinity (Lee et al. 2018; Wu et al. 2009).

Since cellulose has constrained thermal stability, TEMPO modified cellulose was able to experience thermal degradation and decomposition at lower temperatures. This quality is auspicious for low temperature processing techniques, such as drug delivery system (Rostamitabar et al. 2021). Additionally, with the reduced thermal stability of cellulose, it has necessitated less energy to initiate thermal decomposition in the modified cellulose. This energy-saving aspect contributes to more environmentally friendly manufacturing process and lessen the entire adverse impacts of modified cellulose.

Dispersion stability test

Figure 5 shows the image suspension of cellulose before and after TEMPO oxidation in vial. The stability of the cellulose for all samples was then investigated using UV-vis absorbance analysis. As stated by Zainith and Mishra (2021), the accumulation of sediments in the liquid at the bottom of the container is expected as a visual indicator of the sample stability. Based on Figure 6, the stability of the sample is analysed within 90 minutes. From the spectrum below, C2-TEMPO is observed to have the highest stability where the stability reached at 45 minutes, followed by C1-TEMPO where the stability reached at 55 minutes. It has previously been noted that water-soluble oxidized products are unlikely to develop in the case of native celluloses due to the high crystallinity of C1 (Isogai et al. 1998). The UV-vis absorption analysis is proved that after TEMPO-modification, the suspensions do not readily agglomerate and therefore, their dispersion states do not significantly alter when they are stored. This statement can be strengthened further by the outcomes of the discussion in FESEM morphology section, where Figure 1(d) displays scattered structure, which can help improve the dispersion of the cellulose. Throughout the stability study, we are able to forecast its functionality and usefulness for numerous applications. It can be used in several industrial processes and research purposes since it helps improve dispersion stability, and ensures the finished product's stability, evenness and homogeneity (Njuguna et al. 2015; Rajendran et al. 2022).

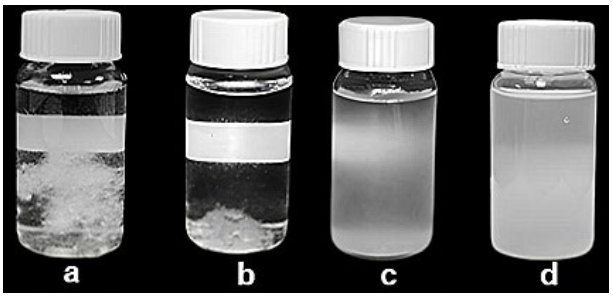

Figure 5: Dispersion analysis of (a) C1; (b) C2; (c) C1-TEMPO; (d) C2-TEMPO.

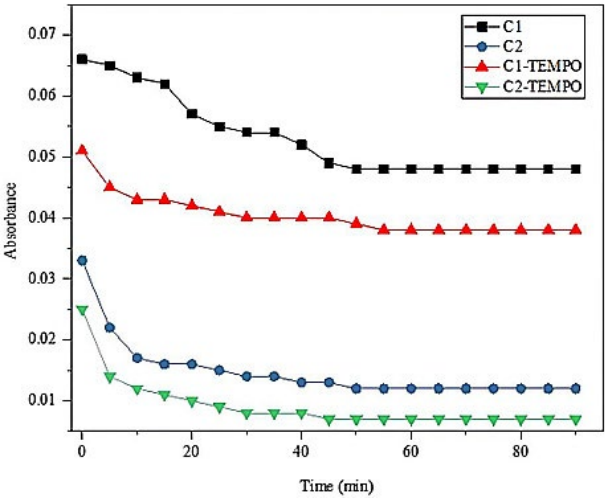

Figure 6: Spectrum of UV-vis absorption of sample C1; C2; C1-TEMPO and C2-TEMPO.

CONCLUSION

Native cellulose has been successfully modified by mercerization (NaOH/urea) and oxidation (TEMPO) processes. The resulting cellulose II (C2) shows changed in crystallinity, molecular weight, and other properties, which may be useful for a variety of applications. However, the benefits of dispersing C2 in water was unsuccessful. Therefore, TEMPO-mediated oxidation was studied for C1 and C2 specifically, due to their different molecular orientation and arrangement of hydrogen bond network. In this study, C1-TEMPO and C2-TEMPO were found had successfully modified the cellulose properties chemically and physically. The presence of the carboxylate group (-COOH) resulting from the oxidation of the primary hydroxyl group (-OH) on cellulose shows that the modification of TEMPO on cellulose was successful, with increasing hydrophilicity towards water. The low crystallinity observed in XRD for cellulose with TEMPO modified suggests that TEMPO technique has disrupted the regular arrangement of the cellulose chains. However, no changed was observed on the crystallinity of C2-TEMPO which demonstrated that only amorphous regions of C2 were exposed to the reaction not the crystalline

areas. The dispersed structure observed using FESEM morphological analysis indicates that C2-TEMPO helps to improve cellulose dispersion by generating more dispersed and separated cellulose fiber structures due to TEMPO-modification. In order to attempt the dispersibility of cellulose I (C1) and cellulose II (C2) by TEMPO-mediated oxidation, C2-TEMPO shows a better dispersion effect compared to C1-TEMPO. This is also proven in the dispersion analysis results, where C2-TEMPO shows the highest stability and the best dispersion effect compared to all samples. A high degree of cellulose dispersion can improve the quality of the final product. For example, TEMPO-modified cellulose can be crosslinked with cross-linking agents to create cellulose hydrogels for use in agricultural and biomedical applications such as control release fertilizer and tissue engineering, respectively. This improves the properties of the material and ensures successful integration into the desired materials.

AUTHORSHIP CONTRIBUTION

Project Idea: NAG, KMS, NFJ, KAMK, SZ, NHAH

Database: NAG, KMS, NFJ, KAMK, SZ, NHAH

Funding: NAG, KMS, NFJ, KAMK, SZ, NHAH

Processing: NAG, KMS, NFJ, KAMK, SZ, NHAH

Analysis: NAG, KMS, NFJ, KAMK, SZ, NHAH

Writing: NAG, KMS, NFJ, KAMK, SZ, NHAH

Review: NAG, KMS, NFJ, KAMK, SZ, NHAH

ACKNOWLEDGEMENT

A wreath of gratitude is given to the Ministry of Higher Education (KPT) Malaysia for support through the Research Grant project, LRGS/1/2019/UKM-UKM/5/1 and Universiti Kebangsaan Malaysia (UKM). The authors warmly recognise the Center for Research and Instrumentation Management (CRIM) UKM and the Faculty of Science and Technology, UKM for their facility and equipment provided throughout the study.

REFERENCES

ALVES, L.; MEDRONHO, B.; ANTUNES, F. E.; et al. Dissolution state of cellulose in aqueous systems. 1. Alkaline solvents. *Cellulose* v.23, n.1, p. 247–258, 2015.

AZIZ, T.; FARID, A.; HAQ, F.; et al. A Review on the Modification of Cellulose and Its Applications. MDPI.: 2022.

BAJPAI, P. Structure of Lignocellulosic Biomass. *Pretreatment of Lignocellulosic Biomass* , hlm. p.7–12, 2016.

BARON, R. I.; COSERI, S. Preparation of water-soluble cellulose derivatives using TEMPO radical-mediated oxidation at extended reaction time. *Reactive and Functional Polymers* v.157, 104768, 2020.

BECK, S.; BOUCHARD, J.; BERRY, R. 2012. Dispersibility in water of dried nanocrystalline cellulose. *Biomacromolecules* v.13, n.5, p. 1486–1494.

CHAKA, K. T. Extraction of cellulose nanocrystals from agricultural by-products: a review. Taylor and Francis Ltd.:v.15, n. 3, p.582-597 2022.

COSERI, S.; BILIUTA, G.; ZEMLJIČ, L. F.; et al. One-shot carboxylation of microcrystalline cellulose in the presence of nitroxyl radicals and sodium periodate. *RSC Advances* v.5, n.104, p. 85889–85897, 2015.

FUKUZUMI, H.; SAITO, T.; OKITA, Y.; et al. Thermal stabilization of TEMPO-oxidized cellulose. *Polymer Degradation and Stability* v.95, n.9, p. 1502–1508, 2010.

GAN, S.; PADZIL, F. N. M.; ZAKARIA, S.; et al. Synthesis of liquid hot water cotton linter to prepare cellulose membrane using NaOH/urea or LiOH/urea. *BioResources* v.10, n.2, p. 2244–2255, 2015a.

GAN, S.; ZAKARIA, S.; CHIA, C. H.; CHEN, R. S.; ELLIS, A. V.; KACO, H. Highly porous regenerated cellulose hydrogel and aerogel prepared from hydrothermal synthesized cellulose carbamate. *PLOS ONE* v.12, n.3, p.1–13, 2017.

GAN, S.; ZAKARIA, S.; CHIA, C. H.; et al. Effect of graphene oxide on thermal stability of aerogel bio-nanocomposite from cellulose-based waste biomass. *Cellulose* v.25, n.9, p. 5099–5112, 2018.

GAN, S.; ZAKARIA, S.; CHIA, C. H.; et al. Effect of hydrothermal pretreatment on solubility and formation of kenaf cellulose membrane and hydrogel. *Carbohydrate Polymers* v.115, p. 62–68, 2015b.

GAN, S.; ZAKARIA, S.; NG, P.; et al. Effect of acid hydrolysis and thermal hydrolysis on solubility and properties of oil palm empty fruit bunch fiber cellulose hydrogel. *BioResources* v.11, n.1, p.126–139, 2016.

GAO, L.; SHI, S.; HOU, W.; et al. NaOH/Urea swelling treatment and hydrothermal degradation of waste cotton fiber. *Journal of Renewable Materials* v.8, n.6, p. 703–713, 2020.

GHAZALI, N. A.; SALLEH, K. M.; JAFRI, N. F.; et al. Potensi Sungkup Plastik daripada Filem Selulosa Terjana Semula: Suatu Ulasan. Penerbit Universiti Kebangsaan Malaysia. v. 51, n.9, p.3043-3057, 2022.

GUBITOSI, M.; NOSRATI, P.; HAMID, M. K.; et al. Stable, metastable and unstable cellulose solutions. *Royal Society Open Science* v.4, n.8, 2017.

HASTUTI, N.; KANOMATA, K.; KITAOKA, T. Characteristics of TEMPO-Oxidized Cellulose Nanofibers from Oil Palm Empty Fruit Bunches Produced by Different Amounts of Oxidant. *IOP Conference Series: Earth and Environmental Science* v.359, n.1, 2019.

HIROTA, M.; FURIHATA, K.; SAITO, T.; et al. Glucose/glucuronic acid alternating co-polysaccharides prepared from TEMPO-oxidized native celluloses by surface peeling. *Angewandte Chemie - International Edition* v.49, n.42, p. 7670–7672, 2010.

ILHAM, Z. Biomass classification and characterization for conversion to biofuels. *Value-Chain of Biofuels: Fundamentals, Technology, and Standardization*: p.69–87, 2022.

ISOGAI, A.; AND, Ã.; KATO, Y. Preparation of polyuronic acid from cellulose by TEMPO-mediated oxidation. Japan, v.5, p.153-164, 1998.

ISOGAI, A.; SAITO, T.; FUKUZUMI, H. TEMPO-oxidized cellulose nanofibers. *Nanoscale* v.3, n.1, p. 71–85, 2011.

JOSEPH, B.; SAGARIKA, V. K.; SABU, C.; et al. Cellulose nanocomposites: Fabrication and biomedical applications. *Journal of Bioresources and Bioproducts* v.5, n.4, p. 223–237, 2020.

KAFFASHSAIE, E.; YOUSEFI, H.; NISHINO, T.; et al. Direct conversion of raw wood to TEMPO-oxidized cellulose nanofibers. *Carbohydrate Polymers*, v.262 -117938, 2021.

KRASSIG, H. A. Cellulose: Structure, Accessibility and Reactivity. *Journal of polymer science. Part A: Polymer Chemistry* v.32, n.1, p. 2401,1994.

LEE, H.; SUNDARAM, J.; ZHU, L.; et al. Improved thermal stability of cellulose nanofibrils using low-concentration alkaline pretreatment. *Carbohydrate Polymers* v.181, p. 506–513, 2018.

MAZLAN, N. S. N.; ZAKARIA, S.; GAN, S.; et al. Comparison of regenerated cellulose membrane coagulated in sulphate based coagulant. *Cerne* v.25, n.1, p. 18–24, 2019.

MEDRONHO, B.; LINDMAN, B. Competing forces during cellulose dissolution: From solvents to mechanisms. Elsevier Ltd.,v. 19, n. 1, p.32-40, 2014.

MHD HANIFFA, M. A. C.; CHING, Y. C.; CHUAH, C. H.; et al. Effect of TEMPO-oxidization and rapid cooling on thermo-structural properties of nanocellulose. *Carbohydrate Polymers* v.173, p. 91–99, 2017.

MILANOVIC, J.; SCHIEHSER, S.; POTTHAST, A.; et al. Stability of TEMPO-oxidized cotton fibers during natural aging. *Carbohydrate Polymers* v.230, p. 115587, 2020.

NAGARAJAN, S.; SKILLEN, N. C.; IRVINE, J. T. S.; et al. Cellulose II as bioethanol feedstock and its advantages over native cellulose. *Renewable and Sustainable Energy Reviews* v.77, p. 182–192, 2017.

NAM, S.; FRENCH, A. D.; CONDON, B. D.; et al. Segal crystallinity index revisited by the simulation of X-ray diffraction patterns of cotton cellulose Iβ and cellulose II. *Carbohydrate Polymers* v.135, p. 1–9, 2016.

NJUGUNA, J.; VANLI, O. A.; LIANG, R. A Review of Spectral Methods for Dispersion Characterization of Carbon Nanotubes in Aqueous Suspensions. Hindawi Publishing Corporation.: 2015a.

NJUGUNA, J.; VANLI, O. A.; LIANG, R. A Review of Spectral Methods for Dispersion Characterization of Carbon Nanotubes in Aqueous Suspensions. Hindawi Publishing Corporation.: 2015b.

NUNES, R. C. R. Rubber nanocomposites with nanocellulose. *Progress in Rubber Nanocomposites*: p.463–494, 2017.

OKITA, Y.; SAITO, T.; ISOGAI, A. Entire surface oxidation of various cellulose microfibrils by TEMPO-mediated oxidation. *Biomacromolecules* v.11, n.6, p.1696–1700, 2010.

PADZIL, F. N. M.; ZAKARIA, S.; CHIA, C. H.; et al. Effect of acid hydrolysis on regenerated kenaf core membrane produced using aqueous alkaline-urea systems. *Carbohydrate Polymers* v.124, p. 164–171, 2015.

PUANGSIN, B.; YANG, Q.; SAITO, T.; et al. Comparative characterization of TEMPO-oxidized cellulose nanofibril films prepared from non-wood resources. *International Journal of Biological Macromolecules* v.59, p. 208–213, 2013.

RAJENDRAN, D.; RAMALINGAME, R.; ADIRAJU, A.; et al. Role of Solvent Polarity on Dispersion Quality and Stability of Functionalized Carbon Nanotubes. *Journal of Composites Science* v.6, n.1, 2022.

ROHAIZU, R.; WANROSLI, W. D. Sono-assisted Tempo oxidation of oil palm lignocellulosic biomass for isolation of nanocrystalline cellulose. *Ultrasonics Sonochemistry* v.34, p. 631–639, 2017.

ROSTAMITABAR, M.; SUBRAHMANYAM, R.; GURIKOV, P.; et al. Cellulose aerogel micro fibers for drug delivery applications. *Materials Science and Engineering C* v.127, 2021.

RUBENTHEREN, V.; WARD, T. A.; CHEE, C. Y.; et al. Effects of heat treatment on chitosan nanocomposite film reinforced with nanocrystalline cellulose and tannic acid. *Carbohydrate Polymers* v.140, p. 202–208, 2016.

SAITO, T.; NISHIYAMA, Y.; PUTAUX, J. L.; et al. Homogeneous suspensions of individualized microfibrils from TEMPO-catalyzed oxidation of native cellulose. *Biomacromolecules* v.7, n.6, p.1687–1691, 2006.

SAWADA, D.; NISHIYAMA, Y.; SHAH, R.; et al. Untangling the threads of cellulose mercerization. *Nature Communications* v.13, n.6189, 2022.

SEGAL, L.; CREELY, J. J.; MARTIN, A. E. et al. An Empirical Method for Estimating the Degree of Crystallinity of Native Cellulose Using the X-Ray Diffractometer. *Textile Research Journal*: v. 29, n. 10, p.786–794, 1959.

SHEN, X.-J.; HUANG, P.-L.; CHEN, J.-H.; et al. Comparison of Acid-hydrolyzed and TEMPO-oxidized Nanocellulose for Reinforcing Alginate Fibers. *BioResources* v.12, n.4, p. 8180–8198, 2017.

SHRIVASTAVA, A. Polymerization. *Introduction to Plastics Engineering*: 17–48, 2018.

TANG, Z.; LI, W.; LIN, X.; et al. TEMPO-Oxidized cellulose with high degree of oxidation. *Polymers* v.9, n.9, p. 3–4, 2017.

WANG, Q.; LIU, S.; CHEN, H.; et al. TEMPO-Oxidized Cellulose Beads for Cationic Dye Adsorption. *Cellulose microbead adsorption* v.17, n.4, p. 6056–6066, 2022.

WANG, Y.; DENG, Y. The kinetics of cellulose dissolution in sodium hydroxide solution at low temperatures. *Biotechnology and Bioengineering* v.102, n.5, p. 1398–1405, 2009.

WEI, Q. Y.; LIN, H.; YANG, B.; et al. Structure and Properties of All-Cellulose Composites Prepared by Controlling the Dissolution Temperature of a NaOH/Urea Solvent. *Industrial and Engineering Chemistry Research* v.59, n.22, p. 10428–10435, 2020.

WU, R. L.; WANG, X. L.; LI, F., et al. Green composite films prepared from cellulose, starch and lignin in room-temperature ionic liquid. *Bioresource Technology* v.100, n.9, p. 2569–2574, 2009.

XIE, K.; TU, H.; DOU, Z.; et al. The effect of cellulose molecular weight on internal structure and properties of regenerated cellulose fibers as spun from the alkali/urea aqueous system. *Polymer* v.215, 2021.

YANG, Q.; QIN, X.; ZHANG, L. Properties of cellulose films prepared from NaOH/urea/zincate aqueous solution at low temperature. *Cellulose* v.18, n.3, p. 681–688, 2011.

ZAINITH, P.; MISHRA, N. K. Experimental Investigations on Stability and Viscosity of Carboxymethyl Cellulose (CMC)-Based Non-Newtonian Nanofluids with Different Nanoparticles with the Combination of Distilled Water. *International Journal of Thermophysics* v.42, n.10, 2021.

ZHANG, H.; LUAN, Q.; HUANG, Q.; et al. A facile and efficient strategy for the fabrication of porous linseed gum/cellulose superabsorbent hydrogels for water conservation. *Carbohydrate Polymers* v.157, p. 1830–1836, 2017a.

ZHANG, H.; XU, Y.; LI, Y.; et al. Facile cellulose dissolution and characterization in the newly synthesized 1,3-diallyl-2-ethylimidazolium acetate ionic liquid. *Polymers* v.9, n.10, 2017b.

ZHAO, D.; LIU, M.; REN, H.; et al. Dissolution of cellulose in NaOH based solvents at low temperature. *Fibers and Polymers* v.14, n.8, p. 1261–1265, 2013.

ZHAO, G.; DU, J.; CHEN, W.; et al. Preparation and thermostability of cellulose nanocrystals and nanofibrils from two sources of biomass: rice straw and poplar wood. *Cellulose* v.26, n.16, p. 8625–8643, 2019.

ZHOU, L.; KE, K.; YANG, M. B. et al. Recent progress on chemical modification of cellulose for high mechanical-performance Poly(lactic acid)/Cellulose composite: A review. *Composites Communications* v.23, 2021.